IJEMD-M, 02 (01) (2023), 1-11 https://doi.org/10.54938/ijemdm.2023.02.1.200

International Journal of Emerging Multidisciplinaries:

Mathematics

Research Paper

Journal Homepage: https://www.ijemd.com

ISSN (print): 2790-1998, ISSN (online): 2790-3257

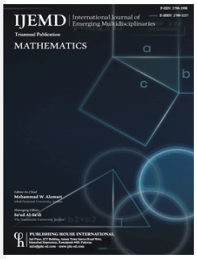

Effect of Cattaneo-Christov model over a vertical stretching cylinder using SiO_2 nanofluid

Zaffer Elahi[1*], Maimoona Siddiqua[1] and Azeem Shahzad[1]

[1]*Department of Basic Sciences, University of Engineering and Technology, Taxila -47050, Pakistan*

[*]*Corresponding author*

Abstract

This paper represents the heat transfer of SiO_2 nanofluid over a vertical stretching cylinder. By using, suitable transformations, the governing partial differential equations are changed into non-linear ordinary differential equations, which are then solved by the numerical solver namely BVP4C. The scrutinized results both in the form of graphical and numerically have been developed from the scheme BVP4C. By using pictorial graphs, the physical parameter that appear in temperature profile are discussed. Further, the rate of shear-stress and heat transfer at the surface have been computed and tabulated in Tables 3-4.

Keywords: *Heat transfer; SiO_2-nanofluid; Cattaneo-Christov model*

Nomenclature:

κ_f	Thermal conductivity of base fluid $(W/K/m)$
κ_{nf}	Thermal conductivity of nanofluid $(W/K/m)$
C_p	Specific heat of fluid $(J/kg/K)$
Nu	Nusselt number (-)
Re	Reynolds number (-)
B_0	Magnetic field
η	Similarity variable (-)
U_w	Surface velocity (m/s)
α, c	Dimensional constants (S^{-1})
α_f	Thermal diffusion of base fluid (m^2/s)
α_{nf}	Thermal diffusivity of nanofluid (m^2/s)
ρ_{nf}	Density of nanofluid (kg/m^3)
μ_f	Dynamic viscosity of base fluid $(kg\ m/s)$
μ_{nf}	Dynamic viscosity of nanofluid $(kg\ m/s)$
ν_f	Kinematic viscosity of base fluid (m^2/s)
ν_{nf}	Kinematic viscosity of nanofluid (m^2/s)
σ_{nf}	Electrical conductivity of nanofluid (-)
$(\rho C_p)_{nf}$	Heat capacity of nanofluid (-)

***Email addresses*: zaffer.elahi@uettaxila.edu.pk (Z. Elahi), maimoona.siddiqua@students.uettaxila.edu.pk (M. Siddiqua), azeem.shahzad@uettaxila.edu.pk (A. Shahzad)**

Received 02.02.2023; Published 30.05.2023

1. Introduction

The heat transfer is an important phenomenon due to its wide application in the fields of engineering and industrial areas, such as the cooling of nuclear reactors, heat exchangers, refrigerators, air coolers, and generation of energy. The heat transfer occurs due to the temperature difference between two neighboring objects. The Fourier proposed the law of heat conduction to determine the behavior of heat transfer in many different experimental setups [1]. The drawback of this model is a parabolic form of the equation that reveals the whole substance is instantly affected by initial disturbance. To remove this drawback Cattaneo suggested modified Fourier's law by introducing the thermal relaxation time parameter yields the hyperbolic form of the equation for heat transfer resulting transfer of heat has finite speed in the entire medium [2]. Christov [3] presented modified Cattaneo model with thermal relaxation time parameter along with Oldroyd′s upper convected derivative to achive the material invarient formulation. Straughan [4] analyze the Cattano-Christov model with thermal convection in horizontal layer of an incompressible Newtonian fluid. Ciarletta and Straughan [5] discussed the structural stability and uniqueness of the Cattaneo-Christov model. Tribullo and Zampoli [6] studied the uniqueness of Cattaneo Christov heat flux model of an incompressible fluid flow. Han *et al.* [7] presented the heat transfer of viscoelastic fluid with Cattaneo-Christov model. Makinde *et al.* [8] investigated the combined effects of Brownian motion, thermophoresis and Cattaneo-Christov model of Casson nanofluid boundary layer flow. Upadhya *et al.* [9] explored the magnetohydrodynamic (MHD) flow of viscous fluid with the impact Cattaneo-Christov model over stretching sheet. Khan *et al.* [10]] analyzed the transport of energy in Maxwell fluid flow with the help of Cattaneo-Christov theory over stretching cylinder. Elahi *et al.* [11] focused on heat transfer analysis of nanofluid in a thin liquid film over an unsteady stretching surface. Ali *et al.* [12] emphasizes the thermophysical properties of base fluid with different-shaped Al_2O_3 particles in the heat transfer of an unsteady thin film flow over a stretching layer.

The study of flow and heat transfer of non-Newtonian fluids across a stretching surface has garnered a lot of interest in recent years in engineering problems, such as chemical engineering and particularly, manufacturing of plastic and rubber sheets, hot rolling, continuous cooling, and fibres spinning, lubricants as well as suspension solutions. Ahmed *et al.* [13] proposed MHD axisymmetric flow of power-law fluid over an unsteady stretching sheet with convective boundary conditions. Ahmed *et al.* [14] studied the effects of inclined Lorentz forces on boundary layer flow of Sisko fluid over a radially stretching sheet with radiative heat transfer. Shahzad *et al.* [15] worked on the unsteady axisymmetric flow and heat transfer over time-dependent radially stretching sheet. Ahmed *et al.* [16] studied a note on convective heat transfer of an MHD Jeffrey fluid over a stretching sheet.

The goal of this paper to analyze the impact SiO_2 nanofluid over a vertically stretching cylinder using cattaneo-christov model. The rest of the paper is organized as follows, the modeling of proposed problem is given in section 2. In section 4, the solution methodology of the problem is presented. The graphical as well as numerical result are discussed in section 5. Finally, section 6 is devoted to summarize the finding of the paper.

2. Mathematical Formulation

Consider a vertical stretching cylinder, attached with a slit of radius R acting perpendicularly to the axis of cylinder. The fluid is moving uniform velocity $U_w = \frac{cz}{1-\alpha t}$ in $z-$direction under the intensity of magnetic field B_0 in $r-$direction as shown in Figure 2.1.

Let $u = u(r,z,t)$ and $w = w(r,z,t)$ be the respective velocity components in $r-$ and $z-$direction, and $T = T(r,z,t)$ represents the temperature of the nanofluid. Further, it is assume that the base fluid and multi-shape nanoparticles are in equilibrium. Under these assumption, Tiwari and Das nanofluid model is used to extract the governing equations of continuity, momentum and energy are, as under [17, 18].

$$\frac{\partial(ru)}{\partial r} + \frac{\partial(rw)}{\partial z} = 0, \tag{1}$$

$$\frac{\partial w}{\partial t} + u\frac{\partial w}{\partial r} + w\frac{\partial w}{\partial z} = \frac{\mu_{nf}}{\rho_{nf}}\frac{\partial(r\frac{\partial w}{\partial r})}{\partial r} + g\beta(T - T_\infty) - \frac{\sigma_{nf}}{\rho_{nf}}B_0^2 w, \tag{2}$$

$$\rho_{nf}C_p\left(\frac{\partial T}{\partial t} + u\frac{\partial T}{\partial r} + w\frac{\partial T}{\partial z}\right) = -\nabla.\mathbf{q} + \mu_{nf}\left(\frac{\partial w}{\partial r}\right)^2, \tag{3}$$

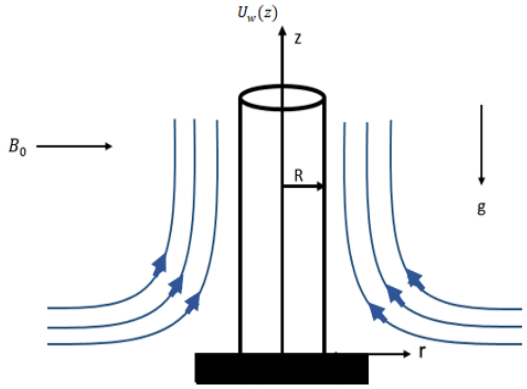

Figure 2.1: Schematic diagram of the problem

Christov [3] and Han *et al.* [7] proposed that the heat flux equation satisfy the following relation

$$q+\lambda_1\left(\frac{\partial q}{\partial t}+V.\nabla\mathbf{q}+(\nabla\mathbf{V})q-q.\nabla\mathbf{V}\right)=-k\nabla\mathbf{T}, \tag{4}$$

where λ_1 is thermal relaxation time, k is the thermal conductivity and V is the velocity vector. In particular, the classical Fourier law is formed for $\lambda_1 = 0$.
Combining (3) and (4), leads to

$$\begin{aligned}\frac{\partial T}{\partial t}+u\frac{\partial T}{\partial r}+w\frac{\partial T}{\partial z}=\frac{\mu_{nf}}{\rho_{nf}C_p}\left(\frac{\partial w}{\partial r}\right)^2+\frac{\alpha_{nf}}{r}\frac{\partial(\frac{\partial T}{\partial r})}{\partial r}+\lambda_1\Bigg[2\mu_{nf}\left(\frac{\partial w}{\partial r}\right)\\ \left(\frac{\partial^2 w}{\partial t\partial r}+u\frac{\partial^2 w}{\partial r^2}\right)-\rho_{nf}C_p\Bigg\{\frac{\partial^2 T}{\partial t^2}+u^2\frac{\partial^2 T}{\partial r^2}+w^2\frac{\partial^2 T}{\partial z^2}+2u\frac{\partial^2 T}{\partial t\partial r}+2w\frac{\partial^2 T}{\partial t\partial z}+\\ 2uw\frac{\partial^2 T}{\partial z\partial r}+\left(\frac{\partial u}{\partial t}+u\frac{\partial u}{\partial r}+w\frac{\partial u}{\partial z}\right)\frac{\partial T}{\partial r}+\left(\frac{\partial w}{\partial t}+u\frac{\partial w}{\partial r}+w\frac{\partial w}{\partial z}\right)\frac{\partial T}{\partial r}\Bigg\}\Bigg],\end{aligned} \tag{5}$$

subject to

$$\begin{aligned}u=0,\ \ w=U_w,\ \ \frac{\partial T}{\partial r}=0\quad at\quad r=R,\\ w\to 0,\ \ T\to T_\infty\quad as\quad r\to\infty,\end{aligned} \tag{6}$$

where h_f is the convective heat transfer coefficient.
The thermophysical properties of nanofluids are defined as follows [19, 20].

$$\left.\begin{aligned}\alpha_{nf}=\frac{\kappa_{nf}}{(\rho C_p)_{nf}},\rho_{nf}=(1-\phi)\rho_f+\phi\rho_s,\mu_{nf}=\mu_f(1+A_1\phi+A_2\phi^2),\\ \sigma_{nf}=\sigma_f(1-\phi)\sigma_f+\phi\sigma_s,(\rho C_p)_{nf}=(1-\phi)(\rho C_p)_f+\phi(\rho C_p)_s,\end{aligned}\right\} \tag{7}$$

and

$$\frac{\kappa_{nf}}{\kappa_f}=\left[\frac{\kappa_s+(m-1)\kappa_f+(m-1)(\kappa_s-\kappa_f)\phi}{\kappa_s+(m-1)\kappa_f-(\kappa_s-\kappa_f)\phi}\right], \tag{8}$$

The thermophysical properties of base fluid and SiO_2 nanofluid are given in Table 1.
While, the values of viscosity coefficients A_1, A_2 and shape factor m of multi-shape nps of SiO_2 nanofluid are given in Table 2.

Table 1: Thermophysical properties of base fluid and SiO_2 nanofluid [21]

nps/ Base water	Density (kg/m^3)	Thermal conductivity $(W/m\,K)$	Specific heat $(J/kg\,K)$	Electric conductivity (S/m)
SiO_2	2200	1.2	703	5.5×10^{-6}
H_2O	997.1	0.613	4179	5.50

Table 2: Viscosity and shape factor of nps [22, 23]

	Platelet	Cylinder	Sphere
A_1	37.1	13.5	2.5
A_2	612.6	904.4	6.5
m	5.72	4.82	3.0

3. Dimensionless Model

Introducing the similarity variable as follows [24, 25],

$$\theta(\eta)=\frac{T-T_\infty}{T_\omega-T_\infty},\eta=\left(\frac{c}{\nu_f(1-\alpha t)}\right)^{\frac{1}{2}}\left(\frac{r^2-R^2}{2R}\right),\psi=\left(\frac{c\nu_f}{1-\alpha t}\right)^{\frac{1}{2}}zRf(\eta), \tag{9}$$

where the flow pattern ψ is defined as $u=-\frac{1}{r}\frac{\partial\psi}{\partial z}$ and $w=\frac{1}{r}\frac{\partial\psi}{\partial r}$, that satisfy the continuity equation (1) directly.
Using the similarity variables defined in (9), the momentum Eqn.(2) and energy Eqn.(5) with boundary condition (6) lead to

$$\varepsilon_1(1+2\kappa\eta)f'''(\eta)+2\varepsilon_1\kappa f''(\eta)-\varepsilon_3Mf'(\eta)+\left[f(\eta)f''(\eta)-f'^2(\eta)-S\left(f'(\eta)+\frac{\eta}{2}f''(\eta)\right)\right]+\lambda\theta(\eta)=0, \tag{10}$$

$$(1+2\kappa\eta)\left(\varepsilon_1Ec\,f''^2(\eta)+\frac{\varepsilon_2}{Pr}\theta''(\eta)\right)+\frac{2\varepsilon_2}{Pr}\kappa\theta'(\eta)-S\left(2\theta(\eta)+\frac{\eta}{2}\theta'(\eta)\right)+f(\eta)\theta'(\eta)-$$

$$f'(\eta)\theta(\eta)+\beta_1\left[\varepsilon_1Ec(1+2\kappa\eta)\left(3Sf''^2(\eta)+S\eta f''(\eta)f'''(\eta)-2f(\eta)f''(\eta)f'''(\eta)\right)-\right.$$

$$2\varepsilon_1Ec\kappa f(\eta)f''^2(\eta)-\left\{S^2\left(6\theta(\eta)+\frac{11}{4}\eta\theta'(\eta)+\frac{\eta^2}{4}\theta''(\eta)\right)+S\left(5f'(\eta)\theta(\eta)-\frac{11}{2}f\eta\theta'(\eta)\right.\right.$$

$$\left.-\eta f(\eta)\theta''(\eta)+(\eta-\frac{1}{2})f'(\eta)\theta'(\eta)+\frac{\eta}{2}f''(\eta)\theta(\eta)\right)+f^2(\eta)\theta''(\eta)-f(\eta)f'(\eta)\theta'(\eta)$$

$$\left.\left.-f(\eta)f''(\eta)\theta(\eta)+f'^2(\eta)\theta(\eta)\right\}\right]=0, \tag{11}$$

subject to

$$\begin{aligned}f(\eta)=0,f'(\eta)=1,\theta(\eta)-1=0at\,\eta=0,\\ f'(\eta)\to0,\theta(\eta)\to0as\eta\to\infty.\end{aligned} \tag{12}$$

where

- $\kappa=\frac{1}{R}\left(\frac{\nu_f(1-\alpha t)}{c}\right)^{\frac{1}{2}}$ is the Curvature parameter,

- $\gamma = \frac{h_f}{k_{nf}} \left(\frac{\nu_f z}{U_w}\right)^{\frac{1}{2}}$ is the Biot-number,
- $Ec = \frac{U_w^2}{C_p(T_w - T)}$ is the Eckert number,
- $M = \frac{\beta_0 \sigma_f (1-\alpha t)}{c \rho_{nf}}$ is the magnetic parameter,
- $Pr = \frac{(\rho\ C_p)_f\ \nu_f}{\kappa_f}$ is the Prandtl number,
- $\lambda = \frac{g\beta(1-\alpha t)^2 (T_w - T_\infty)}{c^2 z}$ is the mixed convection parameter,
- $S = \frac{\alpha}{c}$ is the unsteadiness parameter,
- $\beta_1 = \frac{c\lambda_1}{1-\alpha t}$ is the thermal relaxation parameter.

The constants $\varepsilon_i,\ i = 1, \ldots, 3$ are used in (10) and (11), defined as

$$\varepsilon_1 = \frac{1 + A_1\phi + A_2\phi^2}{1 - \phi + \phi\left(\frac{\rho_s}{\rho_f}\right)},\ \ \varepsilon_2 = \frac{\left(\frac{\kappa_{nf}}{\kappa_f}\right)}{1 - \phi + \phi\frac{(\rho C_p)_s}{(\rho C_p)_f}},\ \ \varepsilon_3 = \frac{1 - \phi + \phi\left(\frac{\sigma_s}{\sigma_f}\right)}{1 - \phi + \phi\left(\frac{\rho_s}{\rho_f}\right)}, \tag{13}$$

where ϕ is the solid volume fraction parameter.
The rate of shear-stress and strain at the surface of vertically stretched cylinder can be defined, as

$$C_f = \frac{2\tau_w}{\rho_f\ U_w^2} = \frac{2\mu_{nf}}{\rho_f\ U_w^2}\ \left[\frac{\partial u}{\partial r}\right]_{r=R}, \tag{14}$$

and

$$Nu = -\frac{z\kappa_{nf}}{\kappa_f\ (T_w - T_\infty)} \left[\frac{\partial T}{\partial r}\right]_{r=R}. \tag{15}$$

In non-dimensional form (14) and (15) can be written, as

$$\frac{1}{2} Re^{\frac{1}{2}} C_f = (1 + A_1\phi + A_2\phi^2)\ f''(0) and Re^{-\frac{1}{2}} Nu = -\frac{\kappa_{nf}}{\kappa_f}\ \theta'(0). \tag{16}$$

4. Method of Solution

The numerical scheme BVP4C has been used to determine the solution of nonlinear system of equations (10-12) by considering

$$\begin{aligned}
f &= y_1, && (17)\\
y_1' &= y_2, && (18)\\
y_2' &= y_3, && (19)\\
y_3' &= g_1, && (20)\\
y_4 &= \theta, && (21)\\
y_4' &= y_5, && (22)\\
y_5 &= g_2, && (23)\\
y_4(\eta) - 1 &= 0,\ \ y_1(\eta) = 0,\ \ y_2(\eta) = 1, at\, \eta = 0, && (24)\\
y_2 &\to 0,\ \ y_4 \to 0 as \eta \to \infty. && (25)
\end{aligned}$$

where

$$g_1 = \frac{1}{\varepsilon_1(1 + 2\eta\kappa)} \left[\varepsilon_3\, M y_2 - 2\varepsilon_1 \kappa y_3 - \lambda y_4 - \left\{y_1 y_3 - y_2^2 - S\left(y_2 + \frac{\eta}{2} y_3\right)\right\}\right], \tag{26}$$

and

$$g_2 = \frac{4Pr}{4(1+2\kappa\eta)\varepsilon_2 - Pr\beta_1\left(S^2\eta^2 - 4S\eta\, y_1 + 4y_1^2\right)}\Big[S\left(2y_4 + \frac{\eta}{2}y_5\right) - y_1y_5 + y_2y_4 - \left(\frac{2\varepsilon_2\kappa y_5}{Pr}\right)$$
$$-(1+2\kappa\eta)\varepsilon_1 Ec\, y_3^2 - \beta_1\Big\{\varepsilon_1 Ec(1+2\kappa\eta)\left(3Sy_3^2 + S\eta y_3y_3' - 2y_1y_3y_3'\right) - 2\varepsilon_1 Ec\kappa y_1y_3^2 + y_1y_2y_5$$
$$+y_1y_3y_4 - y_2^2y_4 - \frac{S^2}{4}\left(24y_4 + 11\eta y_5\right) - \frac{S}{2}\left\{10y_2y_4 - 11y_1y_5 + (2\eta-1)y_2y_5 + \eta\, y_3y_4\right\}\Big\}\Big]. \qquad (27)$$

Solving the system of first order equation (17-23) together with (24-25) using BVP4C packages Matlab. The obtained result have been presented graphically and in tabular form in the following section.

5. Results and Discussion

This article focus on the analysis of the behavior of the Cattaneo-Christov model for SiO_2 nanofluid past over a vertical stretching cylinder. In this section, the effects of pertinent features of physical parameter have been plotted graphically and elucidate in detail. Particularly, the numerically computation of Skin friction and Nusselt number have been done for each shape of nps in tabular form.

5.1. Graphical Results

Figure 6.1 shows the effect of thermal relaxation time parameter for multi-shape nps. In each case of multi-shape nps, the temperature field is getting decreased by continuously varying the β_1 values. Physically, immediate propagation of heat waves in a medium is controlled by larger values of relaxation parameter in Cattaneo-Christov model. As a result, the fluid with increasing relaxation parameter values require more time to heat transfer. Consequently, the temperature profile decreases.

In Figure 6.2 the impact of Ec on temperature profile is sketched for multi-shape nps. The higher values of Eckert number Ec enhance the temperature profile for each multi-shape nanoparticles. Eckert number illustrated the relative contribution of kinetic energy dissipated to the boundary layer enthalpy difference. For $Ec = 0$, there is no viscous dissipation. As Ec increases, there is a progressively greater conversion of kinetic energy to heat which results in an elevation in temperatures.

Figure 6.3 demonstrates the effect of curvature κ on the temperature profile for multi-shape nps. For higher values of curvature parameter κ , we noted increasing trend in temperature field for each case of multi-shape nps. Physically, higher values of curvature parameter κ reduces the surface area of cylinder thus the boundary layer thickness increases.

5.2. Numerical Results

The skin friction coefficient has been computed, for each shape of nps by varying the physical parameters numerically in Table 3. It is observed the decrease in volume-fraction ϕ, magnetic field M and unsteadiness parameter S, for each shape of nps.

Table 3: Skin-friction coefficient of multi-shape nps

Physical	parameters		Platelet	Cylinder	Sphere
ϕ	M	S		$-Re^{\frac{1}{2}}C_f$	
0.00	1.0	0.4	1.1888753	1.1888753	1.18887530
0.01	-	-	1.4690596	1.3383205	1.20343350
0.02	-	-	1.7825431	1.5842068	1.21864720
0.02	**0.0**	0.4	1.2310815	1.0799844	0.80428231
-	**1.0**	-	1.7825431	1.5842068	1.21864720
-	**2.0**	-	2.2248785	1.9885355	1.55037650
0.02	1.0	**0.2**	1.6678474	1.4779898	1.12967100
-	-	**0.3**	1.7267806	1.5326233	1.17550930
-	-	**0.4**	1.7825431	1.5842068	1.21864720

Moreover, the rate of heat transfer is getting increase with growing values of Prandtl number, volume-fraction ϕ, and thermal relaxation time parameter in Table 4.

Table 4: Nusselt number of multi-shape nps

Physical	parameters		Platelet	Cylinder	Sphere
ϕ	Pr	β		$Re^{-\frac{1}{2}}Nu$	
0.00	6.0	0.10	0.88922039	1.8820855	1.8820855
0.02	-	-	0.83173994	1.7086404	1.9181955
0.04	-	-	0.77363303	1.4784477	1.9514380
0.02	**4.0**	0.10	1.45932270	1.5389300	1.7096006
-	**6.0**	-	1.61260630	1.7086404	1.9181955
-	**8.0**	-	1.72671090	1.8350857	2.0740675
0.02	6.0	**0.00**	1.38771370	1.4825089	1.6884246
-	-	**0.05**	1.50255050	1.5979736	1.8057281
-	-	**0.10**	1.61260630	1.7086404	1.9181955

6. Conclusion

The manipulation of heat transfer development on Cattaneo-Christov model of silica nanofluid over a vertical stretching cylinder has been done in this article. The pertinent perspective of the propose problem have been performed using BVP4C on Matlab. The key finding of the article have been summarized in the following lines:

- Heat transfer increases with the increasing values of thermal relaxation time parameter β_1.
- The skin friction coefficient decreases for volume-fraction ϕ, magnetic field M and unsteadiness parameter S.
- The Nusselt number increases for the Prandtl number, volume-fraction and thermal relaxation parameter.

References

[1] B. De. Fourier and J. B. Joseph, *The Analytical Theory of Heat*, The University Press, (1878).
[2] C. Christov, On heat conduction, *Atti Sem. Mat. Fis.* Univ. Modena Reggio Emilia, **3** (1948), 83-101.
[3] C. I. Christov, On frame indifferent formulation of the Maxwell–Cattaneo model of finite-speed heat conduction, *Mechanics Research Communications*, **36**(4) (2009), 481-486.
[4] B. Straughan, Thermal conductive with Cattaneo-Christov model, *Int. J. Heat and Mass transfer*, **53** (2010), 95-98.
[5] M. Ciarletta and B. Straughan, Uniqueness and structural stability for the Cattaneo–Christov equations, *Mechanics Research Communications*, **37**(5) (2010), 445-447.
[6] V. Tibullo and V. Zampoli, A uniqueness result for the Cattaneo–Christov heat conduction model applied to incompressible fluids, *Mechanics Research Communications*, **38**(1) (2011), 77-79.
[7] S. Han, L. Zheng, C. Li and X. Zhang, Coupled flow and heat transfer in viscoelastic fluid with Cattaneo–Christov heat flux model, *Applied Mathematics Letters*, **38** (2014), 87-93.
[8] O. D. Makinde, V. Nagendramma, C. S. K. Raju, and A. Leelarathnam, Effects of Cattaneo-Christov heat flux on Casson nanofluid flow past a stretching cylinder, *In Defect and Diffusion Forum*, **378** (2017), 28-38.
[9] S. M. Upadhya, Mahesha and C. S. K. Raju, Cattaneo-Christov heat flux model for magnetohydrodynamic flow in a suspension of dust particles towards a stretching sheet, *Nonlinear Engineering*, **7**(3) (2018), 237-246.
[10] M. khan, A. Ahmed, M. Irfan and J. Ahmed, Analysis of Cattaneo-Christov theory for unsteady flow of Maxwell fluid over stretching cylinder, *Journal of Thermal Analysis and Calorimetry*, **144** (2021), 145-154.
[11] Z. Elahi, M. T. Iqbal and A. Shahzad, Numerical Simulation of Heat Transfer Development of Nanofluids in a Thin Film over a Stretching Surface, *Brazilian Journal of Physics*, **52** (2) (2022), 1-13.
[12] R. Ali, A. Shahzad, K. Saher, Z. Elahi and T. Abbas The thin film flow of Al_2O_3 nanofluid particle over an unsteady stretching surface, *Case Studies in Thermal Engineering*, **29** (2022), 101-695.
[13] J. Ahmed, A. Begum, A. Shahzad and R. Ali, MHD axisymmetric flow of power-law fluid over an unsteady stretching sheet with convective boundary conditions, *Results in Physics*, **6** (2016), 973-981.
[14] J. Ahmed, A. Shahzad, A. Begum, R. Ali and N. siddiqui Effects of inclined Lorentz forces on boundary layer flow of Sisko fluid over a radially stretching sheet with radiative heat transfer, *Journal of the Brazilian Society of Mechanical Sciences and Engineering*, **39**(8) (2017), 3039–3050.
[15] A. Shahzad, R. Ali, A. Begum, M. Hussain and M. Kamran Unsteady axisymmetric flow and heat transfer over time-dependent radially stretching sheet, *Alexandria Engineering Journal,* **56**(1) (2017), 35-41.
[16] J. Ahmed, A. Shahzad K. Masood and R. Ali, A note on convective heat transfer of an MHD Jeffrey fluid over a stretching sheet, *AIP advances*, **5**(11) (2015), 117.

[17] R. J. Tiwari and M. K. Das, Heat transfer augmentation in a two-sided lid-driven differentially heated square cavity utilizing nanofluids, *Int. J. Heat Mass Transf.*, **50**(9-10) (2007), 2002-2018.
[18] N.V. Ganesh, B. Ganga, A. K. A. Hakeem, S. Sarayna and R. Kalaivanan, Hydromagnetic axisymmetric slip flow along a vertical stretching cylinder with a convective boundary condition, *St. Petersburg State Polytechnical University Journal, Physics and Mathematics*, **4** (2016), 253.
[19] S. M. Vanaki, H. Mohammad, A. abdollahi and M. Wahid, Effect of nanoparticle shapes on the heat transfer enhancement in a wavy channel with different phase shifts, *Journal of Molecular Liquids*, **196** (2014), 32-42.
[20] R. L. Hamilton and O. K. Crosser, Thermal conductivity of heterogeneous two-component systems, *Industrial & Engineering chemistry fundamentals*, **1**(3) (1962), 187–191.
[21] S. R. Vajjha and K. D. Debendra, Experimental determination of thermal conductivity of three nanofluids and development of new correlations, *Int. J. Heat Mass Transf.*, **52**(21-22) (2009), 4675-4682.
[22] E.V. Timofeeva, J. L. Routbort and D. Singh, Particle shape effects on thermophysical properties of alumina nanofluids, *Journal of Applied Physics*, **106**(1) (2009), 014304.
[23] S. Bibi, Z. Elahi and A. Shahzad, Impacts of different shapes of nanoparticles on SiO_2 nanofluid and heat transfer in a liquid film over a stretching sheet, *Physica Scripta*, **95**(11) (2020), 115-217.
[24] A. Majeed, T. Javed, and S. Shami, Numerical analysis of Walters-B fluid flow and heat transfer over a stretching cylinder, *Canadian Journal of Physics*, **94**(5) (2016), 522-530.
[25] M. W. Maraka, M. K. Ngugi, and P. K. Roy, Similarity solution of unsteady boundary layer flow of nanofluids past a vertical plate with convective heating, *Global Journal of Pure and Applied Mathematics*, **14**(4) (2018), 517-534.

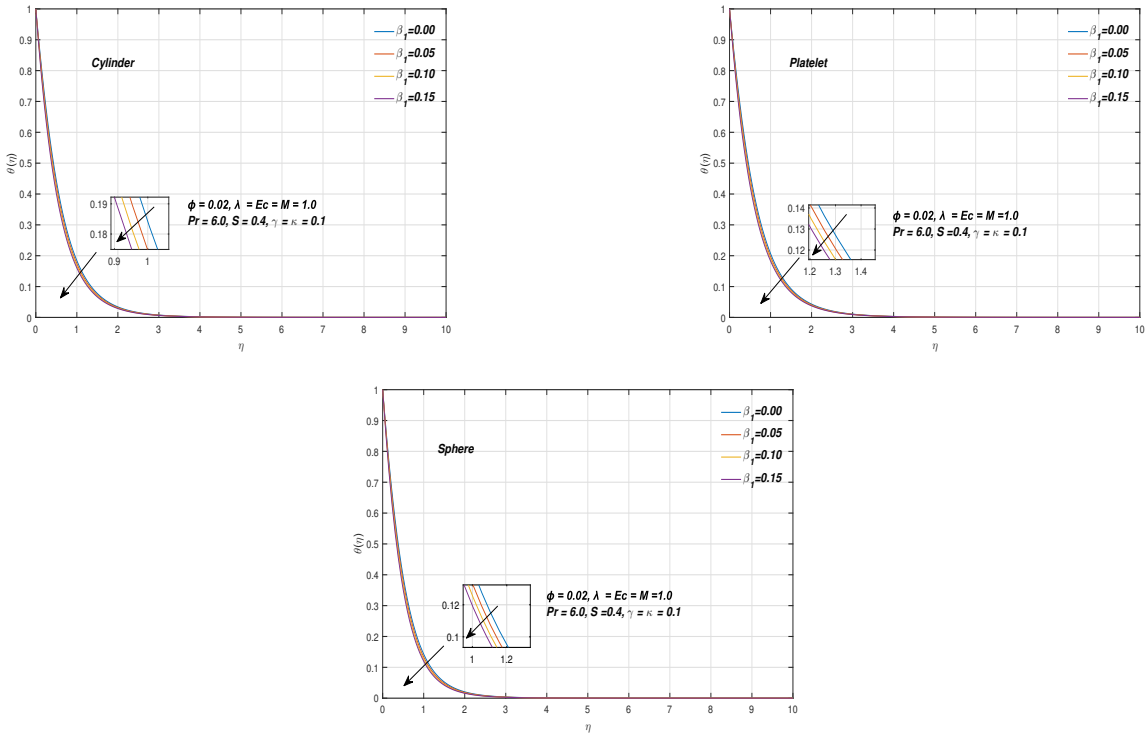

Figure 6.1: Effect of thermal relaxation time parameter β_1 on temperature profile

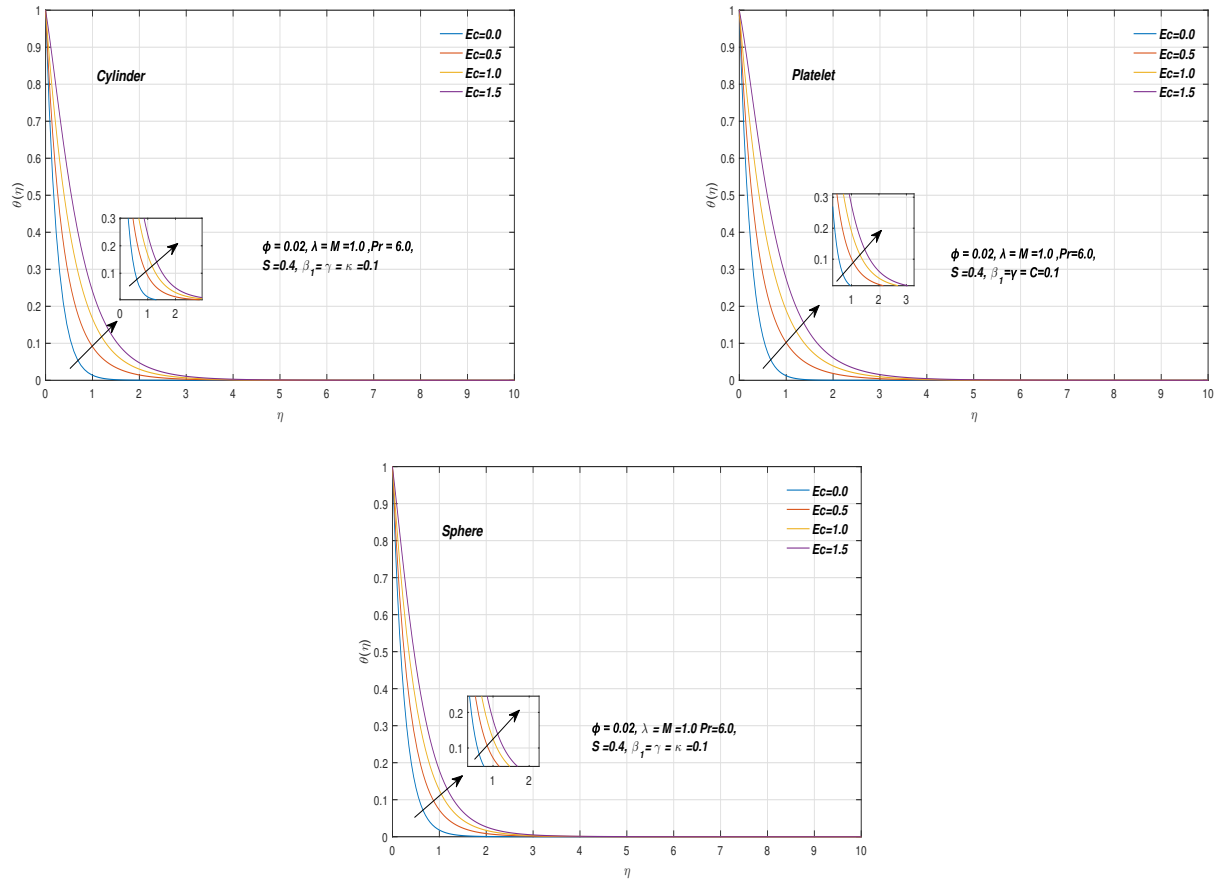

Figure 6.2: Effect of Eckert number (Ec) on temperature profile

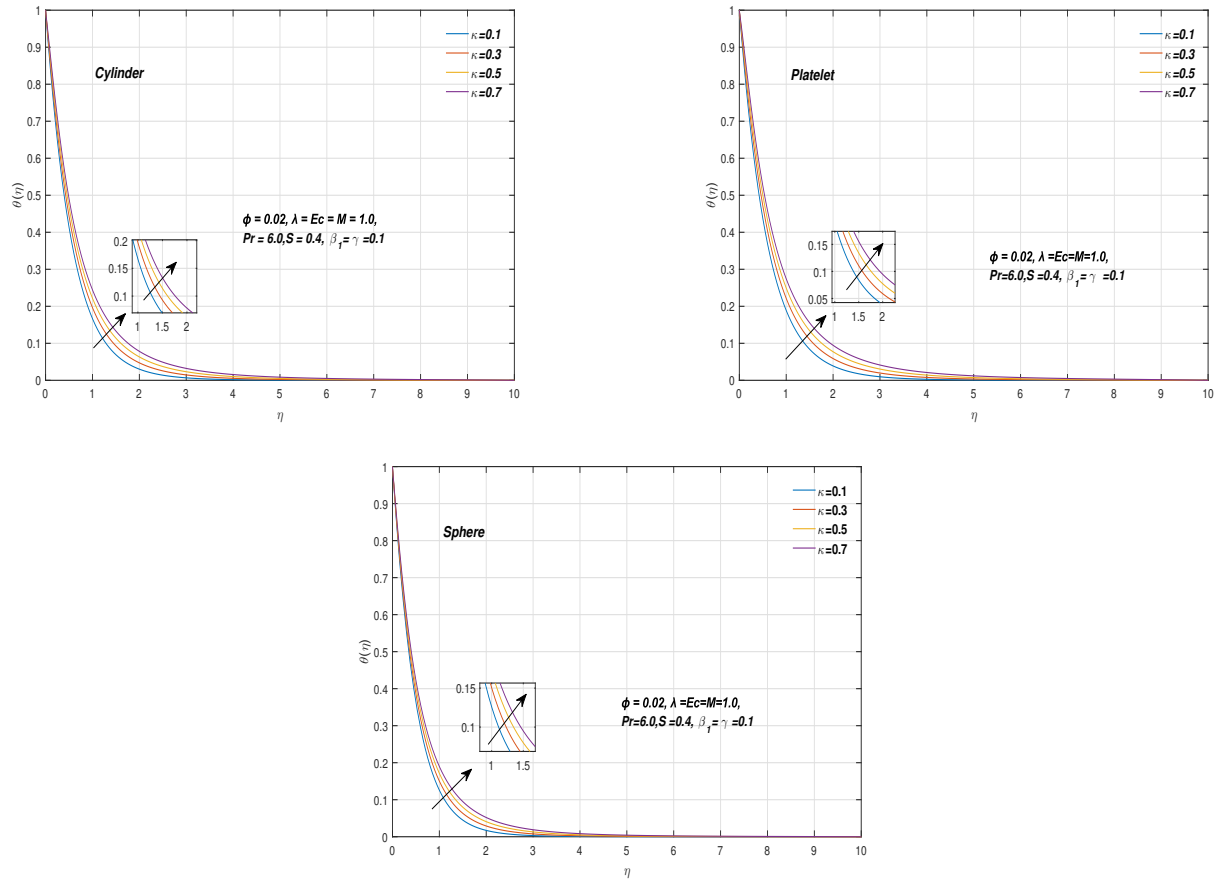

Figure 6.3: Effect of curvature (κ) on temperature profile